Japanese Journal of Applied Physics
Vol. 46, No. 9B, 2007, pp. 6250–6253

Effects of Oxidation during Synthesis on Structure and Field-Emission Property of Tungsten Oxide Nanowires

Yusuke KOJIMA, Keigo KASUYA, Takeshi OOI, Keisuke NAGATO, Kentaro TAKAYAMA, and Masayuki NAKAO

Department of Engineering Synthesis, The University of Tokyo, 7-3-1 Hongo, Bunkyo-ku, Tokyo 113-8656, Japan

(Received November 14, 2006; accepted May 20, 2007; published online September 20, 2007)

We investigated the structure and field-emission property of tungsten oxide nanowires synthesized under different oxidation degrees. We annealed a sputtered tungsten film at 800 °C, controlling the ratio of hydrogen to oxygen (RHO) using Ar/H_2 (97/3%) gas in a vacuum furnace. The resulting differences in shape, number density, length, and width of the nanowires were observed by scanning electron microscopy. In the RHO range of 0 to 0.4, beltlike structures were synthesized. In the RHO range of 0.8 to 4, only thin nanowires were synthesized. In this range, length and width did not differ with RHO, but the number density decreased as RHO increased. The sample with a nanowire density of $2\,\mu m^{-2}$, annealed with an RHO of 4, showed the highest field-emission property, i.e., a current of $1\,mA/cm^2$ for an electric field of $22\,V/\mu m$. We demonstrated their emission by fluorescence imaging and showed that the nanowires are promising candidates for field emitters.
[DOI: 10.1143/JJAP.46.6250]

KEYWORDS: tungsten, tungsten oxide nanowires, oxidation degree, ratio of hydrogen to oxygen (RHO), shape, number density, field-emission property

1. Introduction

Tungsten oxide nanowires are one-dimensional nanostructures, which have diameters of 10–100 nm and a length of about 1 μm. The nanowires spontaneously grow by simple annealing of tungsten materials such as tungsten foils,[1] wires,[2,3] filaments,[4] sputtered films,[5] or powders.[6] Since the nanowires have high aspect ratios and are easily fabricated, they have attracted much attention as promising materials for field emitters.[7–12] Many studies have dwelt on the growth conditions of nanowires. Some studies indicated that the structure of a nanowire is affected by conditions such as oxygen content in tungsten materials.[13] In addition, many researchers investigated the growth mechanism of nanowires. Some studies suggested that the nanowires grow when tungsten oxide molecules diffuse on a material.[14,15] Other studies suggested that the nanowires grow by absorbing tungsten oxide molecules on a material.[16–19] These studies suggested that the growth of nanowires is caused by a migration of tungsten oxide molecule, which is induced by oxidation of the tungsten material. Therefore, the amount of oxygen that reacts with the tungsten material during the synthesis of nanowires should be a factor that affects the morphology of nanowires. However, the effect of the amount of oxygen that reacts with the tungsten material, i.e., oxidation degree, during synthesis of nanowire has not been studied to date.

In this study, we examined the effects of the oxidation degree of tungsten materials during the synthesis of nanowires on their shape, number density, length and width by controlling the ratios of hydrogen to oxygen (RHOs) using an Ar/H_2 mixture gas during annealing for their synthesis. The effect of the oxidation degree on field-emission property, which is affected by the shape and number density of the nanowires, was also clarified using the resulting samples.

2. Experimental Methods

We used sputtered W/Cr films on Si substrates with the thicknesses of 200/50 nm, respectively, as samples. The film was formed by standard radio frequency (rf) magnetron sputtering. The Cr film prevented the tungsten film from detaching from the Si substrates. Ar was used as sputtering gas. The base pressure of the sputtering chamber was 1×10^{-2} Pa and the sputtering pressure was 5×10^{-1} Pa. The deposition rate of tungsten was 13 nm/min. The samples were heated at 200 °C during sputtering to make the film surface smooth. After the deposition, the samples were cooled to room temperature in a vacuum. We placed the samples in a vacuum furnace and annealed them by infrared heating. The base pressure of the furnace was 5 Pa. Keeping the vacuum pump on, we introduced an Ar/H_2 mixture gas (Ar: 97%, H_2: 3%). The flow rate of the mixture gas was varied from 0 to 150 sccm, and the total pressure of the furnace was from 5 to 100 Pa. The leakage rate of the furnace was 2 sccm, which was determined by measuring the increasing pressure rate after shutting off the vacuum pump. Since the ratio of oxygen to air was 0.2, the flow rate of leaking oxygen was estimated to be 0.4 sccm. Therefore, the ratios of hydrogen to oxygen in the furnace were calculated to be 0 to 11 for the Ar/H_2 gas flow rates of 0 to 150 sccm. Each sample was annealed from room temperature up to 800 °C for 10 min and maintained at 800 °C for 10 min. After annealing, we cooled the furnace to room temperature for 30 min while maintaining Ar/H_2 gas flow. The surfaces of these samples were observed by scanning electron microscopy (SEM; Hitachi S-4160). To investigate their field-emission properties, the samples were set with counter-electrodes with a spacing of 75 μm. Their field-emission properties were examined in a chamber evacuated to 1.3×10^{-3} Pa by applying voltage of up to $22\,V/\mu m$ to the electrodes.

3. Results and Discussion

Figures 1(a)–1(f) show SEM images of the surface morphology of the samples annealed with different RHOs. The sample annealed with an RHO of 0 had thick beltlike structures [Fig. 1(a)]. These beltlike structures had widths of 100–500 nm and a length of about 1 μm. For the samples annealed with RHOs of 0.4 and 0.8, the number of beltlike structures decreased and the number of thin nanowires with a high aspect ratio increased with increasing RHO

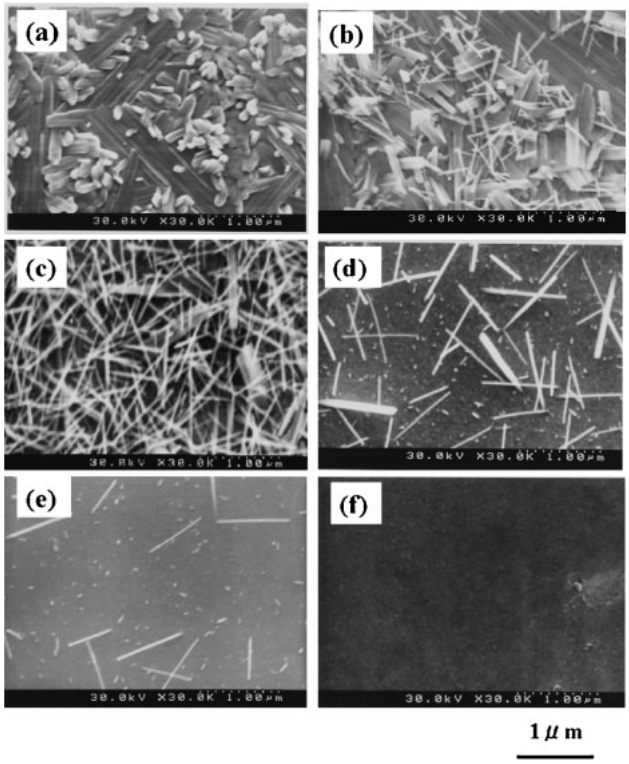

Fig. 1. SEM images of tungsten oxide nanowires annealed at 800 °C with various RHO.

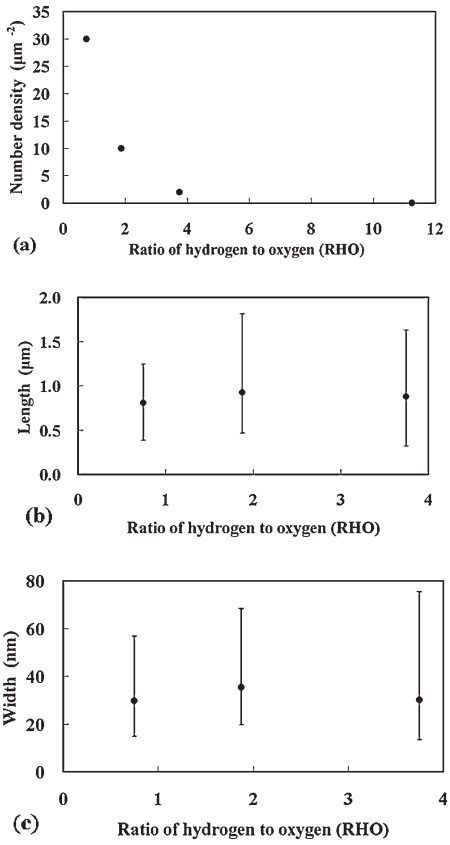

Fig. 2. Relationships between (a) number density, (b) length, and (c) width of nanowires and RHO.

[Figs. 1(b) and 1(c)]. These thin nanowires had diameters of 10–100 nm and a length of about 1 μm. The sample annealed with an RHO of more than 0.8 had only thin nanowires [Figs. 1(c)–1(f)]. Figures 2(a)–2(c) show the relationship between RHO and each of the density, length and width of the nanowires. The samples with only thin nanowires, annealed with an RHO of more than 0.8, were studied. Length and width were averages of measurements of 50 nanowires randomly selected on each sample. The resulting densities of the nanowires on the samples decreased as RHO increased. On the other hand, there were no significant differences in length and width with RHO. These results indicate that only thin nanowires with a high aspect ratio are synthesized in a certain range of the oxidation degree. In this range, the density of nanowires decreases as the oxidation degree of tungsten films decreases and finally the nanowires disappear. Therefore, we can control the number density of nanowires by controlling the oxidation degree of the material using oxidation or reduction gas.

We also investigated the elevation angles of the nanowires from the surface of the sample with an RHO of 2 [Fig. 1(d)] by comparing SEM images of identical nanowires tilted at 0 and 40°. Figure 3(a) shows the number distribution of the elevation angle. The number of nanowires synthesized with an angle range of 40–50° was the largest, and the average angle was 42°. Figure 3(b) shows the relationship between the elevation angle and the length of 150 nanowires randomly selected. The correlation coefficient between the angle and the length was almost 0, indicating that the length has no relationship with the elevation angle.

Figure 4 shows a transmission electron microscopy (TEM; JEM-2010F, JEOL, 200 kV) image of a nanowire

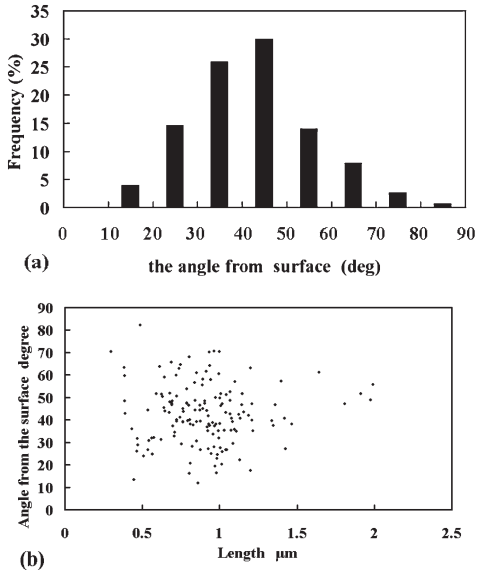

Fig. 3. (a) Number distribution of elevation angle of nanowires. (b) Relationship between elevation angle and length of nanowires for sample annealed with RHO of 2 [shown in Fig. 1(d)]. $N = 150$.

from the sample annealed with an RHO of 0.8 [Fig. 1(c)]. The nanowire had a uniform crystalline structure along the growth direction. The lattice spacing along the growth direction was determined to be 3.64 Å from the electron diffraction (ED) pattern. According to JCPDS card No. 24-747, the growth direction of the nanowire could be identified as monoclinic WO_3[100]. The high-resolution image shows

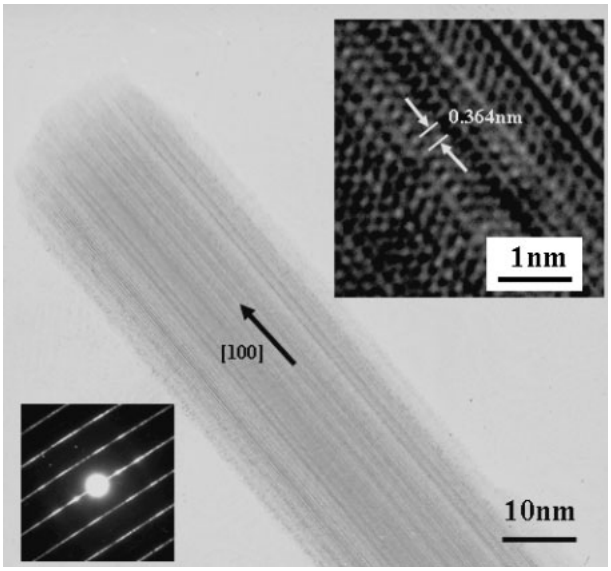

Fig. 4. TEM image of nanowire annealed with RHO of 0.8 [shown in Fig. 1(c)]. The insets show a high-resolution TEM image and an ED pattern of the nanowire.

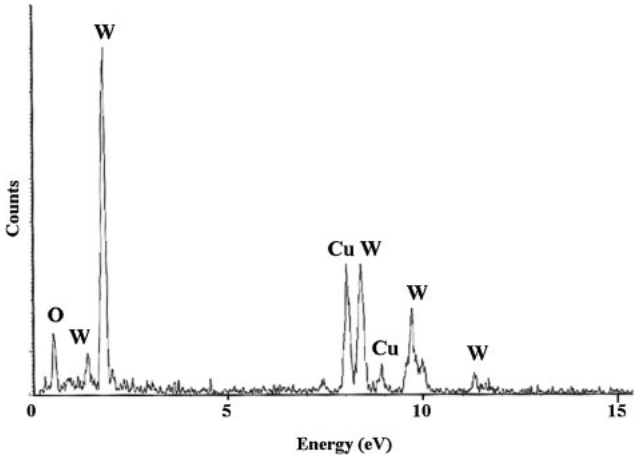

Fig. 5. EDS spectrum of nanowire annealed with RHO of 0.8 [shown in Fig. 1(c)].

that the nanowire also had stacking faults on the growth direction. Li *et al.* have reported that the crystalline structure with stacking faults was different from that without stacking faults.[4] Therefore, we should characterize the crystalline structure of the synthesized nanowires in detail in the future. Figure 5 shows the energy dispersive X-ray spectrometry (EDS) spectrum of the nanowire. The spectrum indicates that the nanowire consists of tungsten and oxygen. The peak of Cu is from the microgrid used for TEM.

We investigated the field-emission properties of the samples with nanowire densities of 30, 10, 2, and $0\,\mu m^{-2}$, annealed with RHOs of 0.8, 2, 4, and 11, respectively [Figs. 1(c)–1(f)]. Figure 6 shows a schematic of the electrodes used for the measurements. These measurements were performed in a vacuum chamber at a pressure of 1.3×10^{-3} Pa. Figure 7 shows the emitted current density of each sample and the Fowler–Nordheim (F–N) plot for the sample with a nanowire density of $2\,\mu m^{-2}$ [the sample shown in Fig. 1(e)]. The F–N plot shows almost a straight line,

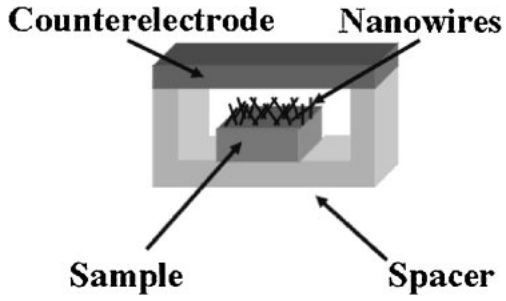

Fig. 6. Schematic of electrodes used for field-emission experiments.

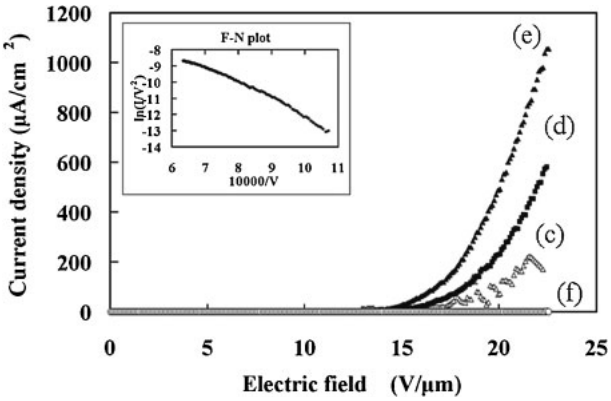

Fig. 7. Relationships between electric field and density of field-emission current: the samples with nanowire densities of (c) 30, (d) 10, (e) 2, and (f) $0\,\mu m^{-2}$, correspond to the samples shown in Figs. 1(c)–1(f), respectively. The inset shows the F–N plot for the sample annealed with an RHO of 4, with a nanowire density of $2\,\mu m^{-2}$ [Fig. 1(e)].

indicating that the current was emitted by field emission. The sample without nanowires hardly emitted any current. On the other hand, the samples with nanowires emitted current. The samples with nanowire densities of 30, 10, and $2\,\mu m^{-2}$ emitted currents of 0.2, 0.6, and $1\,mA/cm^2$ for an electric field of $22\,V/\mu m$, respectively. These results indicate that the samples with a small density emitted a higher current. As reported on carbon nanotubes, many emitters on the substrate shield an electric field from each other and the field-emission property becomes weaker.[20] We assume that the nanowires with a high number density may make field emission difficult. To synthesize nanowires that have a high-field-emission property, the optimal RHO is found to be 4, with which nanowires of $2\,\mu m^{-2}$ are synthesized.

We evaluated the field-emission property of the sample with a nanowire density of $2\,\mu m^{-2}$ [the sample shown in Fig. 1(e)]. The turn-on field, the electric field required to produce a current density of $10\,\mu A/cm^2$, was about $13\,V/\mu m$. According to the F–N theory,[21] the slope of the F–N plot (k) can be described as $k = -6.8 \times 10^7 \varphi^{1.5} d/\beta$, where β is the field-enhancement factor, φ is the work function, and d is the anode–cathode separation. By using the slope value $k = -9884$, the work function of WO_3 $\varphi = 5.7\,eV$,[22] and the anode–cathode separation $d = 7.5 \times 10^{-5}\,m$, β is calculated to be 6.7×10^2. Table I shows the field-enhancement factors and the turn-on field of the nanowires reported by other reserchers. The field-enhancement factor of this work is almost equal to that reported by Lee *et al.*[7] Baek *et al.*[10]

Table I. The field-enhancement factors and turn-on field of the nanowires.

Reference	Field-enhancement factor β	Turn-on field (V/μm)	Pressure (Pa)	Substrate	Composition of nanowire
Lee *et al.*[7] (commented by Bai[21])	7.7×10^2	4.5	1.3×10^{-5}	Flat	W
Zhou *et al.*[8]		2.0	2.7×10^{-5}	Flat	$W_{18}O_{49}$
Li *et al.*[9]		2.6	1.3×10^{-5}	Flat	$W_{18}O_{49}$
Baek *et al.*[10]	1.6×10^3	7.0	1.3×10^{-5}	Tip	W/WO_3
Seelaboyina *et al.*[11]	2.0×10^4	1.2	1.3×10^{-4}	Tip	$W_{18}O_{49}$
Zhou *et al.*[12]		13.85	1.3×10^{-5}	Flat	WO_3
Our work	6.7×10^2	13	1.3×10^{-3}	Flat	WO_3

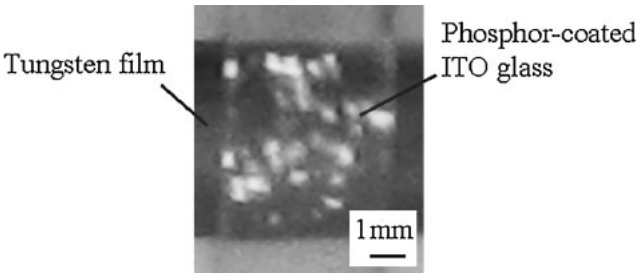

Fig. 8. Fluorescence Image of field emission through phosphor-coated ITO glass for sample annealed with RHO of 4, with a nanowire density of $2\,\mu m^{-2}$ [shown in Fig. 1(e)].

and Seelaboyina *et al.*[11] have a larger field enhancement, which implies that they synthesized the nanowires on a tungsten tip. The turn-on field increases when field emission is performed at a lower vacuum.[11] Therefore, the large turn-on field of this work is attributed to the lower vacuum than those of other studied.

Figure 8 shows a demonstrated field-emission image through phosphor-coated indium tin oxide (ITO) glass for the sample with a nanowire density of $2\,\mu m^{-2}$, annealed with an RHO of 4 [Fig. 1(e)]. This fluorescence image indicates that nanowires are promising candidates for field emitters.

4. Conclusions

We have investigated the shape, number density, length, width and field emission property of tungsten oxide nanowires under different oxidation degrees during their synthesis. We annealed a sputtered tungsten film, controlling RHO by introducing Ar/H_2 gas in a vacuum furnace. In the RHO range of 0 to 0.4, beltlike structures were synthesized. In the RHO range of 0.8 to 4, only thin nanowires were synthesized. In this range, length and width did not differ with RHO, but the number density decreased as RHO increased. The field-emission property of the nanowires increased as the density of the nanowires decreased. The sample with a nanowire density of $2\,\mu m^{-2}$, annealed with an RHO of 4, showed the highest field-emission property, i.e., a current of $1\,mA/cm^2$ for an electric field of $22\,V/\mu m$. We demonstrated their emission by fluorescence imaging and showed that the nanowires are promising candidates for field emitters.

Acknowledgements

This work was supported by Mr. Tsunakawa, Mr. Itoh, and Mr. Ibe of the University of Tokyo for assistance with the TEM image and EDS analysis. We would like to thank Professor Ikuhara and Dr. Shibata of the University of Tokyo for their helpful discussion.

1) Y. Q. Zhu, W. Hu, W. K. Hsu, M. Tarrones, N. Grobert, J. P. Hare, H. W. Kroto, D. R. M. Walton, and H. Terrones: Chem. Phys. Lett. **309** (1999) 327.
2) F. Xu, S. D. Tse, J. F. Al-Sharab, and B. H. Kear: Appl. Phys. Lett. **88** (2006) 243115.
3) Z. Liu, Y. Bando, and C. Tang: Chem. Phys. Lett. **372** (2003) 179.
4) Y. B. Li, Y. Bando, D. Golberg, and K. Kurashima: Chem. Phys. Lett. **367** (2003) 214.
5) M. H. Cho, S. A. Park, K. D. Yang, I. W. Lyo, K. Jeong, S. K. Kang, D. H. Ho, K. W. Kwon, J. H. Ku, S. Y. Choi, and H. J. Shin: J. Vac. Sci. Technol. B **22** (2004) 1084.
6) Y. Z. Jin, Y. Q. Zhu, R. L. D. Whitby, N. Yao, R. Ma, P. C. P. Watts, H. W. Kroto, and D. R. M. Walton: J. Phys. Chem. B **108** (2004) 15572.
7) Y. H. Lee, C. H. Choi, Y. T. Jang, E. K. Kim, and B. K. Ju: Appl. Phys. Lett. **81** (2002) 745.
8) J. Zhou, L. Gong, S. Z. Deng, J. Chen, J. C. She, N. S. Xu, R. Yang, and Z. L. Wang: Appl. Phys. Lett. **87** (2005) 223108.
9) Y. Li, Y. Bando, and D. Golberg: Adv. Mater. **15** (2003) 1294.
10) Y. Baek, Y. Song, and K. Yong: Adv. Mater. **18** (2006) 3105.
11) R. Seelaboyina, J. Huang, J. Park, D. H. Kang, and W. B. Choi: Nanotechnology **17** (2006) 4840.
12) J. Zhou, Y. Ding, S. Z. Deng, L. Gong, N. S. Xu, and Z. L. Wang: Adv. Mater. **17** (2005) 2107.
13) C. H. Chen, S. J. Wang, R. M. Ko, Y. C. Kuo, K. M. Uang, T. M. Chen, B. W. Liou, and H. Y. Tsai: Nanotechnology **17** (2006) 217.
14) C. Klinke, J. B. Hannon, L. Gignac, K. Reuter, and P. Avouris: J. Phys. Chem. B **109** (2005) 17787.
15) J. Pfeifer, E. Badaljan, P. Tekula-Buxbaum, T. Kovacs, O. Geszti, A. L. Toth, and H.-J. Lunk: J. Cryst. Growth **169** (1996) 727.
16) G. Gu, B. Zheng, W. Q. Han, S. Roth, and J. Liu: Nano Lett. **2** (2002) 849.
17) K. Liu, D. T. Foord, and L. Scipioni: Nanotechnology **16** (2005) 10.
18) L. Chi, N. Xu, S. Deng, J. Chen, and J. She: Nanotechnology **17** (2006) 5590.
19) K. Hong, M. Xie, and H. Wu: Nanotechnology **17** (2006) 4830.
20) W. I. Milne, K. B. K. Teo, G. A. J. Amaratunga, P. Legagneux, L. Gangloff, J.-P. Schnell, V. Semet, V. T. Binh, and O. Groening: J. Mater. Chem. **14** (2004) 933.
21) X. Bai and G. Zhang: Appl. Phys. Lett. **88** (2006) 226101.
22) G. Vida, V. K. Josepovits, M. Gyor, and P. Deak: Microsc. Microanal. **9** (2003) 337.